13th World Conference on Earthquake Engineering
Vancouver, B.C., Canada
August 1-6, 2004
Paper No. 24

EVALUATING DISTRIBUTION OF SEISMIC ENERGY IN MULTISTORY FRAMES

Chung-Che CHOU[1] And Chia-Ming UANG[2]

SUMMARY

A simplified procedure similar to the response spectrum method has been developed to estimate the energy absorbed in each mode from energy spectra, and the distribution of energy along frame height is evaluated based on energy shapes established by non-linear modal pushover analysis. The statistics of the estimate of energy are presented for a variety of building frames subjected to ground motion ensembles. The study shows that (1) the proposed procedure which includes the higher mode effects can reasonably predict the total energy and the energy distribution in a structure, (2) the majority of the seismic energy is contributed by the first mode response, and (3) the second-mode energy needs to be considered to predict the damage in the upper stories.

INTRODUCTION

Study on energy demand in single-degree-of-freedom (SDOF) systems is abundant, yet such study on multistory frames is limited. Fajfar and Gašperšič [1] showed that the hysteretic energy demand in a multi-degree-of-freedom (MDOF) system cannot be evaluated reliably from an equivalent SDOF system; they attributed the problem to the higher mode effect. A recent study by Chopra and Goel [2] showed that story drifts along building height can be estimated reliably if more than one equivalent SDOF systems are considered.

The purpose of this study is to present a procedure [3] that can be used to predict the seismic energy demand along the height of a multistory frame without performing a nonlinear time-history analysis. The procedure requires a static pushover analysis of the MDOF system to determine the modal yield force and ductility factor of an equivalent SDOF system for the first few (say, two) modes. After the ductility is determined for each mode, the energy spectrum can be used to determine the contribution of each mode. The absorbed energy of each mode is then distributed along the frame height based on the specific energy shapes, established from the pushover analysis. To verify the procedure, statistics of the SDOF system estimate of absorbed energy are presented for three moment frames and thirty ground motions.

[1] *Assistant Professor, Department of Civil Engineering, National Chiao Tung University, Hsinchu, Taiwan, e-mail: chchou@mail.nctu.edu.tw*
[2] *Professor, Department of Structural Engineering, University of California, San Diego, La Jolla, CA, e-mail: cmu@ucsd.edu*

CONSTANT-DUCTILITY RESPONSE SPECTRA

For an inelastic SDOF system subjected to a ground motion, the energy equation can be derived from the equation of motion [4]:

$$\frac{m(\dot{v}_t)^2}{2} + \int_0^t (c\dot{v})dv + \int_0^t f dv = \int_0^t (m\ddot{v}_t)dv_g \tag{1}$$

or $$E_k + E_\xi + E_a = E_i \tag{2}$$

where v_g, v_t, and v are the ground displacement, total displacement, and relative displacement, respectively. c is the viscous damping coefficient, and f is the restoring force. E_k, E_ξ, and E_i are the kinetic energy, viscous damping energy, and "absolute" input energy, respectively. The absorbed energy, E_a, is composed of the recoverable elastic strain energy and the irrecoverable hysteretic energy. The equivalent velocity of E_a, $V_a = \sqrt{2E_a/m}$, was used as a parameter for energy demand because it converges to the pseudo-velocity in the elastic case. Equivalent velocity V_a was evaluated as the maximum value obtained from a time history analysis with an elastic-perfectly plastic hysteresis model and 5% viscous damping at a given ductility level. For a given ductility factor, the yield force, f_y, can also be normalized by structural weight (mg) as follows: $C_y = f_y/mg$.

Total of thirty ground motions grouped in three sets (ten for each set) are listed in Table 1. The first two sets of motions, representing large magnitude-small distance records, were recorded at sites C and D; the site was classified based on the NEHRP Provisions [5]. The third set of records were developed for the SAC Joint Venture [6]. Typical C_y and V_a response spectra are shown in Figure 1.

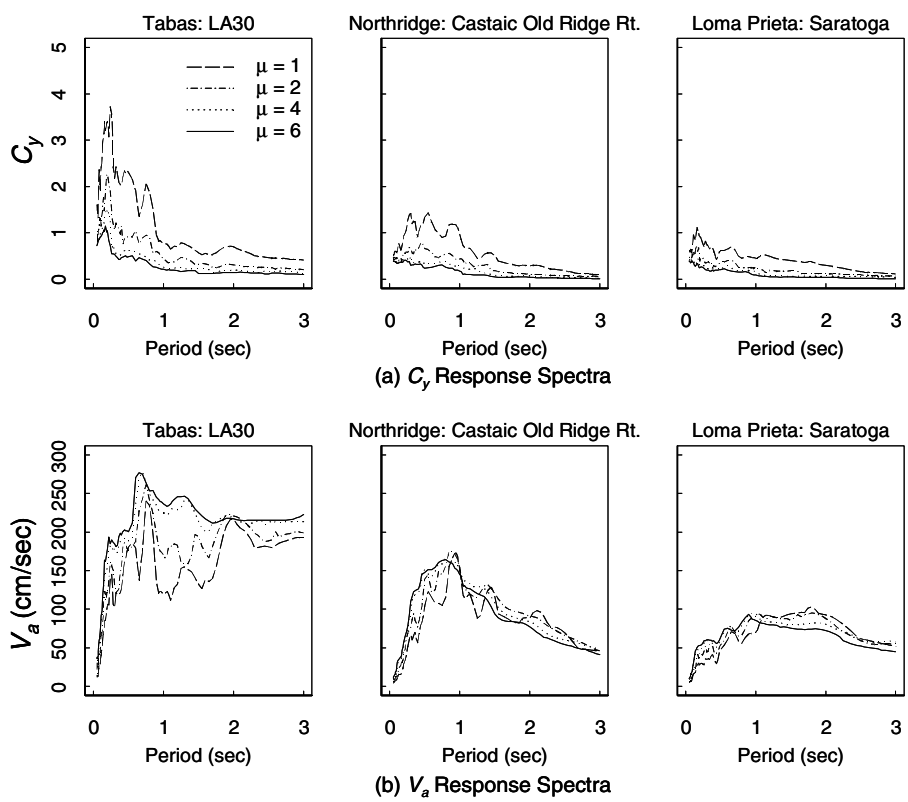

Figure 1 Constant-ductility Spectra

Table 1 Characteristics of Ground Motions

Earthquake Event	Year	M_w	Station or SAC Name	Dist. (km)	Soil Type	Duration (sec)	Scaling Factor	Scaled PGA (cm/s^2)
San Fernando	1971	6.6	Lake Hughes Sta.12	17.0	C	36.7	1.0	346.2
Whittier	1987	6.0	Las Palmas Ave, Glendale	17.8	C	31.5	1.0	299.4
Whittier	1987	6.0	120N. Oakbank, Glendale	16.2	C	32.1	1.0	105.5
Loma Prieta	1989	6.9	Saratoga	11.7	C	40.0	1.0	493.7
Loma Prieta	1989	6.9	Anderson Dam	20.0	C	39.7	1.0	245.4
Loma Prieta	1989	6.9	Santa Cruz	12.5	C	40.0	1.0	433.1
Landers	1992	7.3	Joshua Tree Fire Station	11.3	C	80.0	1.0	278.4
Northridge	1994	6.7	700 N. Faring Rd., LA	14.1	C	34.7	1.0	272.6
Northridge	1994	6.7	Castaic Old Ridge Rt.	20.8	C	60.0	1.0	504.2
Northridge	1994	6.7	Las Palmas Ave, Glendale	17.8	C	37.8	1.0	329.8
Imperial Valley	1979	6.5	El Centro Array #2	16.0	D	71.7	1.0	379.5
Imperial Valley	1979	6.5	Chihuahua	17.7	D	83.6	1.0	261.1
Whittier	1987	6.0	12500 Birchdale, Downey	11.9	D	28.6	1.0	334.0
Whittier	1987	6.0	Castlegate St., Compton	16.5	D	31.2	1.0	312.1
Loma Prieta	1989	6.9	Gilroy Array #4	15.8	D	40.0	1.0	407.9
Loma Prieta	1989	6.9	Gilroy Array #7	24.3	D	40.0	1.0	314.3
Landers	1992	7.3	Yermo	26.3	D	80.0	1.0	240.0
Northridge	1994	6.7	Canyon County	11.4	D	31.0	1.0	446.8
Northridge	1994	6.7	5360 Saturn St., LA	22.3	D	31.6	1.0	433.2
Northridge	1994	6.7	Hollywood Stor. Blg.	20.0	D	46.6	1.0	244.9
Kobe	1995	6.9	LA 22	3.4	-	60.0	1.15	902.8
Loma Prieta	1989	6.9	LA 24	3.5	-	25.0	0.82	463.8
Northridge	1994	6.7	LA 26	7.5	-	60.0	1.29	925.3
Northridge	1994	6.7	LA 28	6.4	-	60.0	1.61	1304.1
Tabas	1974	7.4	LA 30	1.2	-	50.0	1.08	972.6
Elysian Park	-	7.1	LA 32	17.5	-	30.0	1.43	1163.5
Elysian Park	-	7.1	LA 34	10.7	-	30.0	0.97	667.6
Elysian Park	-	7.1	LA 36	11.2	-	30.0	1.1	1079.3
Palos Verdes	-	7.1	LA 38	1.5	-	60.0	0.9	761.3
Palos Verdes	-	7.1	LA 40	1.5	-	60.0	0.88	613.3

ENERGY DEMAND EVALUATION FOR MULTISTORY FRAMES

Modal Response Analysis

To estimate the energy demand of an MDOF system from the V_a spectra, ductility factor of the equivalent SDOF system for each of the first two modes needs to be established first. The procedure includes the following: (1) convert the MDOF system into an SDOF system for each of the first two modes with the corresponding elastic mode shape [7], (2) perform a static pushover analysis to determine the yield strength coefficient, C_y, for each mode, and (3) determine the modal ductility factor from the C_y spectrum. The equation of motion for a planar MDOF system with only lateral degrees of freedom is

$$\mathbf{M}\ddot{\mathbf{v}} + \mathbf{C}\dot{\mathbf{v}} + \mathbf{F} = -\mathbf{M}\mathbf{1}\ddot{v}_g \tag{3}$$

where **M** is the diagonal mass matrix, **C** is the damping matrix, **F** is the restoring force vector in the horizontal direction at each floor, and **1** is an unit vector. $\mathbf{v}$ is a vector of relative displacement and can be expressed as

$$\mathbf{v} = \sum_{n=1}^{N} \boldsymbol{\phi}_n x_n \tag{4}$$

where $\boldsymbol{\phi}_n$ is the elastic mode shape and x_n is the generalized displacement of the n-th mode in an MDOF system. Multiplying both sides of Eq. (4) by $\boldsymbol{\phi}_n^T \mathbf{M}$, the generalized displacement x_n is then calculated as

$$x_n = \boldsymbol{\phi}_n^T \mathbf{M} \mathbf{v} \tag{5}$$

where $\boldsymbol{\phi}_n$ is normalized such that $\boldsymbol{\phi}_n^T \mathbf{M} \boldsymbol{\phi}_n = 1$. Substituting Eq. (4) into Eq. (3) and premultiplying each term by $\boldsymbol{\phi}_n^T$ give

$$\ddot{x}_n + \frac{c_n}{m_n} \dot{x}_n + \frac{f_n}{m_n} = -\boldsymbol{\Gamma}_n \ddot{\mathbf{v}}_g \tag{6}$$

where $\Gamma_n \left(= \boldsymbol{\phi}_n^{\mathrm{T}} \mathbf{M} \mathbf{1} / m_n \right)$ is the participation factor. The generalized restoring force is

$$f_n = \boldsymbol{\phi}_n^T \mathbf{f} \tag{7}$$

To obtain the generalized yield force, f_{yn}, for the n-th mode, a static pushover analysis is performed with the following lateral load:

$$\mathbf{L}_n = \mathbf{M} \boldsymbol{\phi}_n s = \mathbf{q}_n s \tag{8}$$

where $\mathbf{q}_n$ is the lateral load pattern, and s is the scalar factor. At each load step, the generalized force f_n is calculated by premultiplying Eq. (8) by $\boldsymbol{\phi}_n^{\mathrm{T}}$, and the generalized displacement x_n is obtained from Eq. (5) by substituting $\mathbf{v}$ for the resulting lateral displacement vector. Relationships between the generalized force and generalized displacement for the example frames (see Figure 2) are shown in Figure 3. Each curve is then approximated by a bi-linear relationship to determine the generalized yield force, f_{yn}, listed in Table 2. The non-dimensional yield strength coefficient, $\overline{C}_{yn}$, is expressed as $f_{yn} / \Gamma_n m_n g$. Based on $\overline{C}_{yn}$ and period of each mode, the absorbed energy for each of the first two modes is calculated as follows

$$E_{a1} = \frac{1}{2} m_1 \left(V_{a1} \Gamma_1 \right)^2 \tag{9}$$

$$E_{a2} = \frac{1}{2} m_2 \left(V_{a2} \Gamma_2 \right)^2 \tag{10}$$

In order to validate the proposed method, three moment frames with 5-, 7-, and 9-stories in height (see Figure 2) were used in this study. The first two buildings were designed in accordance with the NEHRP Seismic Provisions, and 9-story office building was designed by an SAC-commissioned consulting firm [8]. The calculated frame weight (half of building weight), W, natural periods, T_i, and participation factors of the first two modes are listed in Table 2. The total absorbed energy demands obtained from the MDOF time-history analyses, denoted as E_{am}, are compared with E_{a1} and E_{a2} in the following section.

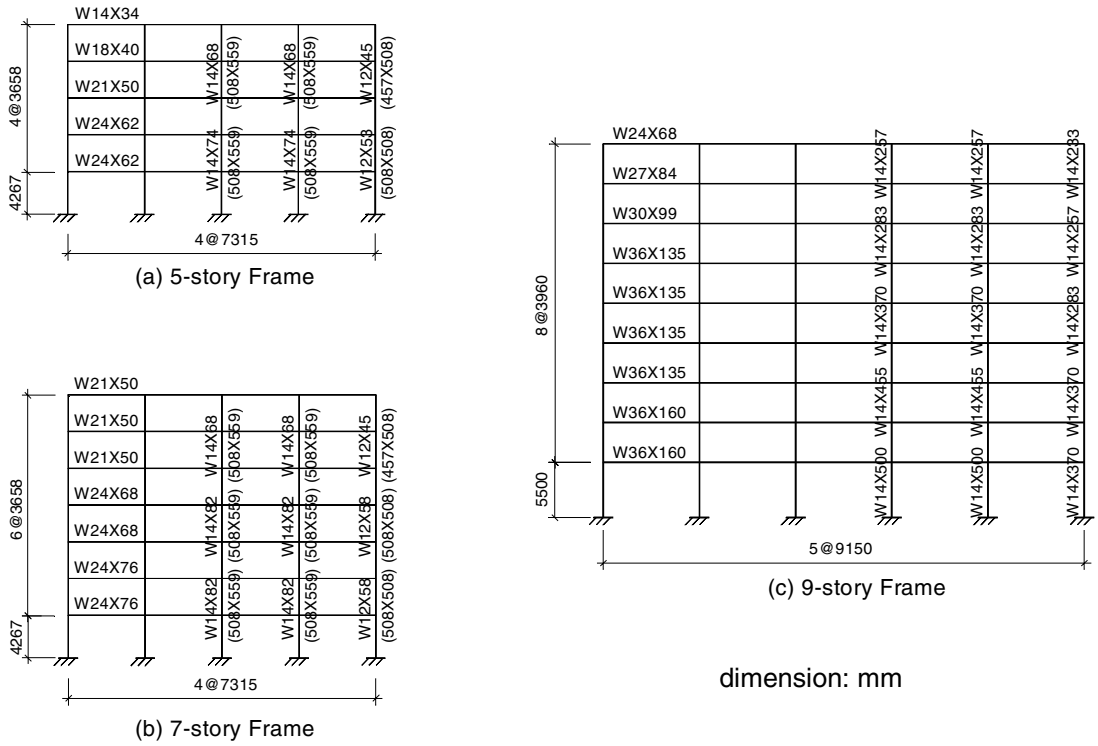

Figure 2 Elevation and Member Sizes of Moment Frames

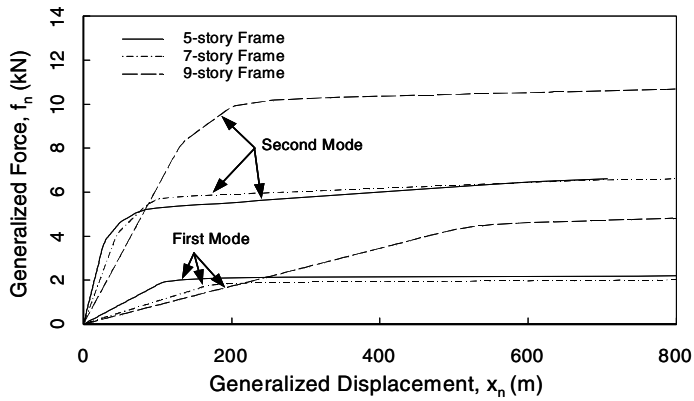

Figure 3 Generalized Force-Generalized Displacement Relationships

Table 2 Frame Properties

Frame	W (kN)	T_1 (sec)	T_2 (sec)	Γ_1	Γ_2	f_{y1} (kN)	f_{y2} (kN)
5-story	7476	1.47	0.53	799.1	295.7	2.15	5.17
7-story	10608	1.85	0.66	952.2	337.6	1.90	5.72
9-story	44214	2.14	0.80	1928.9	696.3	4.81	10.18

Combination Rules and Comparison with Time-History Analysis

The modal information in Table 2 together with the V_a spectra allow for the absorbed energy in each of the first two modes be calculated. The energy quantities then can be combined by using either the absolute sum (ABS) or the square-root-of-sum-of-squares (SRSS) rule. The accuracy of the energy quantities thus computed-denoted as $E_{a,abs}$ and $E_{a,srss}$- is then compared with those predicted by the nonlinear time-history analysis (E_{am}).

The first column in Figure 4 shows that including only the first mode effect would underestimate the total energy demand. The energy ratio, defined as the estimate energy normalized by that computed by non-linear time history analysis, in Figure 5 also shows that such underestimation can be more significant for longer period structures. For yielding structures (i.e., ductility greater than one), both Figures 4 and 5 show that the ABS combination rule provides a better estimation of the energy demand than the SRSS rule.

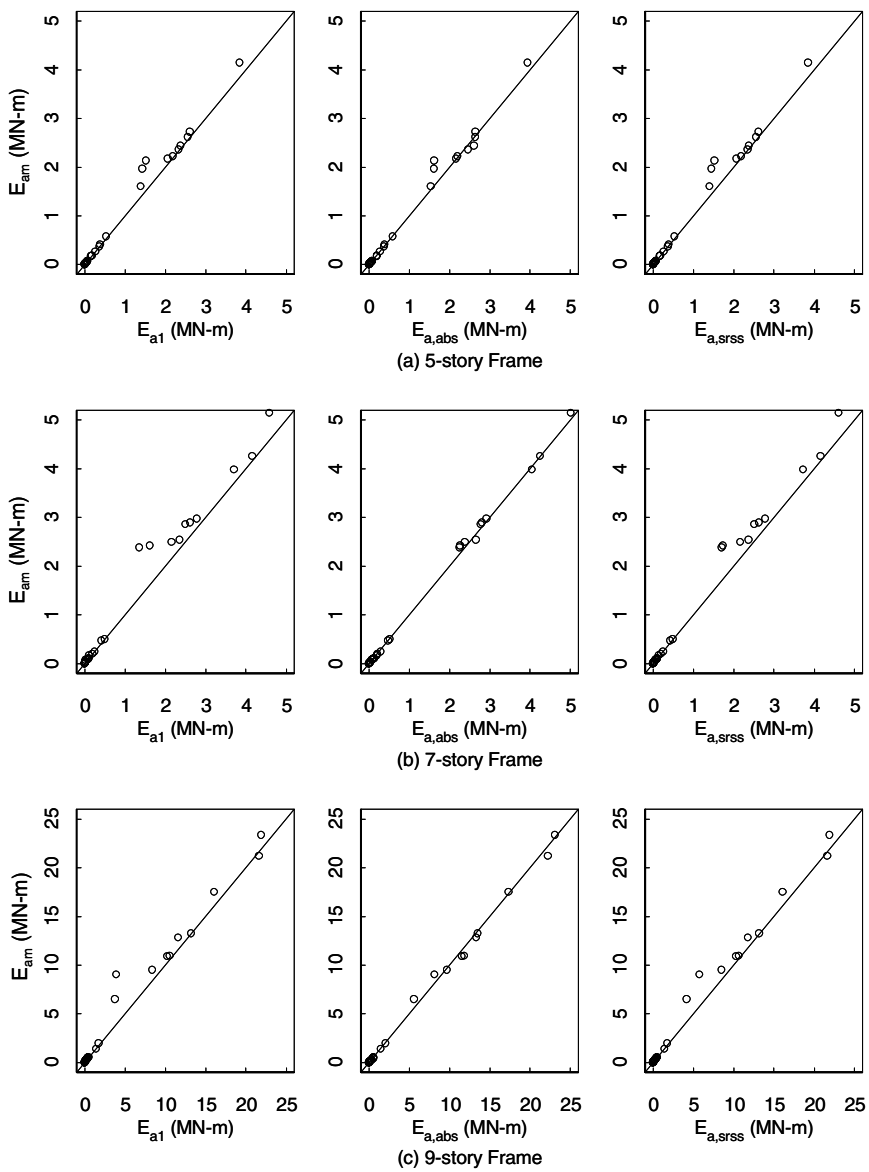

Figure 4 Comparison of Energy Estimation versus Exact Energy Value

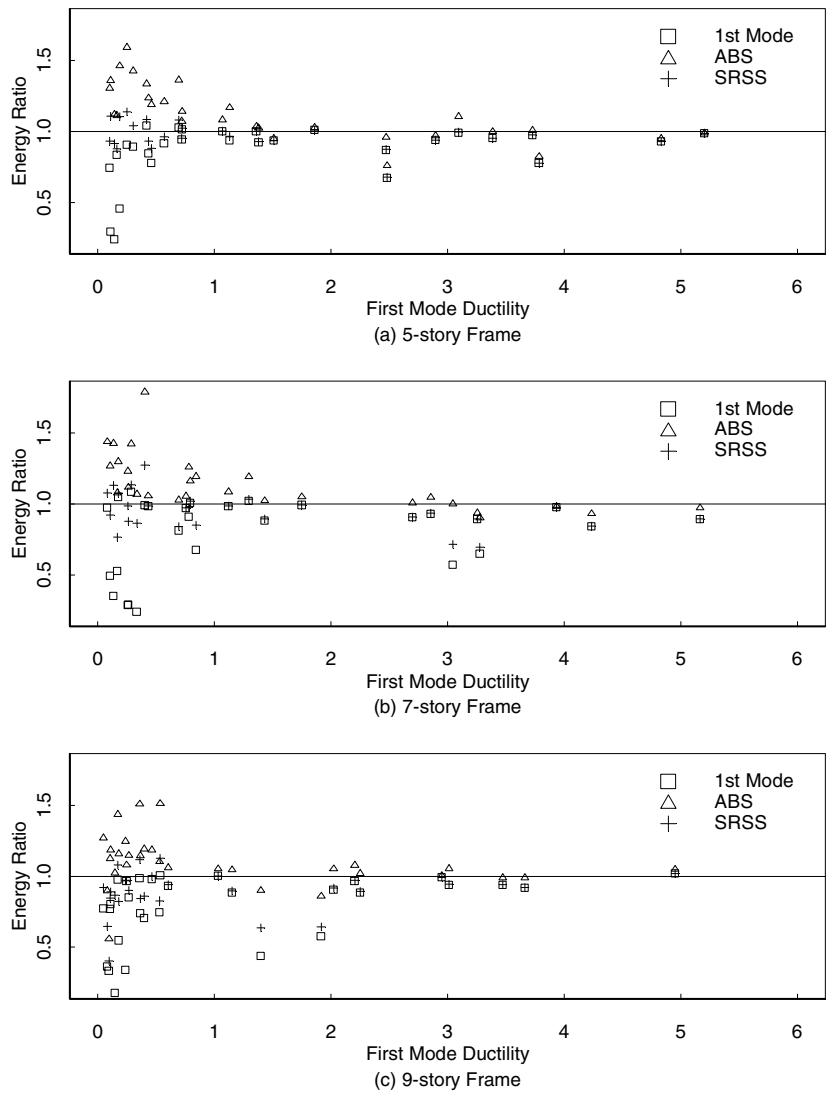

Figure 5 Relationship between Ratio of Estimation and first Mode Ductility

ENERGY DISTRIBUTION EVALUATION IN STRUCTURES

Performing a static pushover analysis based on the first-mode load pattern $\mathbf{q}_1$, Figure 6 shows the relationship between the cumulative rotation, $\eta_{1,\text{base}}$, at the column base and the absorbed energy of each frame. $\eta_{1,\text{base}}$ is the average value of the cumulative rotations at the base of exterior and interior columns. Each column base cumulative rotation is calculated as the absorbed energy normalized by the flexural strength, M_{pc}, of the column. Three zones are characterized from three distinct slopes at load steps A and B, which are shown by solid marks. The first zone (before step A) represents the system within the elastic range. The second zone (between A and B) is typified by the formation of beam plastic hinges at lower floor levels, and the third zone (beyond B) indicates that plastic hinges have formed at the base of the first-story columns. Two limits for the first story drift ratio that corresponds to the initiation of beam yielding (step A) and column base yielding (step B) can be established from the first-mode pushover analysis. $SDR_{1,\text{beam}}$ is the first story drift ratio at step A, and $SDR_{1,\text{base}}$ is the first story drift ratio at step B.

Assuming same beam size on each floor, cumulative rotation in beam $\eta_{1,\text{beam}}$ is calculated as

$$\boldsymbol{\eta}_{1,\text{beam}} = \frac{\sum_{i=1}^{2m} E_{a1,i}}{2mM_{pb}} \tag{11}$$

where m is the number of bays, $E_{a1,i}$ is the absorbed energy in each beam end, and M_{pb} is the beam flexural strength. Three energy shapes ($\boldsymbol{\psi}_1$, $\boldsymbol{\psi}_2$, and $\boldsymbol{\psi}_3$) shown in Figure 7 are obtained by normalizing the beam cumulative rotation on each floor by the second floor's beam rotation.

For a given earthquake ground motion, first story drift ratio SDR_1 produced by the first-mode response can be estimated as follows:

$$SDR_1 = \frac{D_s \boldsymbol{\Gamma}_1 \boldsymbol{\phi}_{11}}{H_1} \tag{12}$$

where H_1 is the first story height, D_s the maximum drift in an SDOF system, is obtained based on the first-mode period and ductility factor, and $\boldsymbol{\phi}_{11}$ is the component of the mode shape $\boldsymbol{\phi}_1$ at the second floor level. Once SDR_1 is calculated, the energy shape for distributing the first- mode energy is determined from the following rule:

$$\text{Shape 1 } (\boldsymbol{\psi}_1) \text{ if } SDR_1 < SDR_{1,\text{beam}} \tag{13}$$

$$\text{Shape 2 } (\boldsymbol{\psi}_2) \text{ if } SDR_{1,\text{beam}} \le SDR_1 < SDR_{1,\text{base}} \tag{14}$$

$$\text{Shape 3 } (\boldsymbol{\psi}_3) \text{ if } SDR_1 \ge SDR_{1,\text{base}} \tag{15}$$

The first-mode energy E_{a1} is then distributed to each floor level and the base of the frame with the chosen energy shape,$\boldsymbol{\psi}_k$. For small levels of strain hardening, the vector of cumulative rotation along the frame height can be determined as

$$\boldsymbol{\eta}_1 = \frac{E_{a1}}{\boldsymbol{\psi}_k^{\mathrm{T}} \hat{\mathbf{M}}_p} \boldsymbol{\psi}_k \tag{16}$$

where $\hat{\mathbf{M}}_p$ is a plastic moment vector, which includes the summation of plastic moment capacities of the columns at the base, and the summation of beam plastic moment capacity.

Performing a pushover analysis with $\mathbf{q}_2$ (= $\mathbf{M}\boldsymbol{\phi}_2$) as the lateral load pattern, Figure 8 shows the relationship between the cumulative rotation, $\eta_{2,\text{base}}$, at the base of the column and the absorbed energy of each frame. $\eta_{2,\text{base}}$ is the average value of the cumulative rotations at the base of exterior and interior columns. Three zones are characterized from three slopes at load steps A and B, which are shown by solid marks. The first zone (before step A) represents the system within the elastic range. The second zone (between A and B) is typified by the formation of beam plastic hinges at upper floor levels, and the third zone (beyond B) indicates that column plastic hinges have formed in the upper floor levels. Normalizing cumulative plastic rotation by its maximum value, three normalized energy shapes ($\overline{\boldsymbol{\psi}}_1$, $\overline{\boldsymbol{\psi}}_2$, and $\overline{\boldsymbol{\psi}}_3$) for each frame are obtained in Figure 9. $\overline{\boldsymbol{\psi}}_1$ is the shape for distributing seismic absorbed energy E_{a2} when the frame responds elastically. $\overline{\boldsymbol{\psi}}_2$ is used as the only shape for distributing E_{a2} for the inelastic case, because shapes $\overline{\boldsymbol{\psi}}_2$ and $\overline{\boldsymbol{\psi}}_3$ are similar. Energy E_{a2} is then distributed to each floor level based on the following expression:

$$\boldsymbol{\eta}_2 = \frac{E_{a2}}{\overline{\boldsymbol{\psi}}_k^{\mathrm{T}} \hat{\mathbf{M}}_p} \overline{\boldsymbol{\psi}}_k \tag{17}$$

where index k can be 1 or 2 determined based on the ductility factor of the second mode. Combining the effects from both modes, the total cumulative rotations in the beams and at the base of the columns are

$$\eta_a = \eta_1 + \eta_2 \tag{18}$$

or

$$\eta_a = \sqrt{\left(\eta_1^2 + \eta_2^2\right)} \tag{19}$$

To verify the procedure, results of three frames subjected to three ground motions are presented. The η_a distributions in Figure 10 show good correlation between the results of MDOF nonlinear time-history analysis and the proposed procedure. The energy absorbed at lower floor levels can be predicted by considering only the first-mode response. However, the second-mode effect is more significant at upper floor levels in the 7- and 9-story frames.

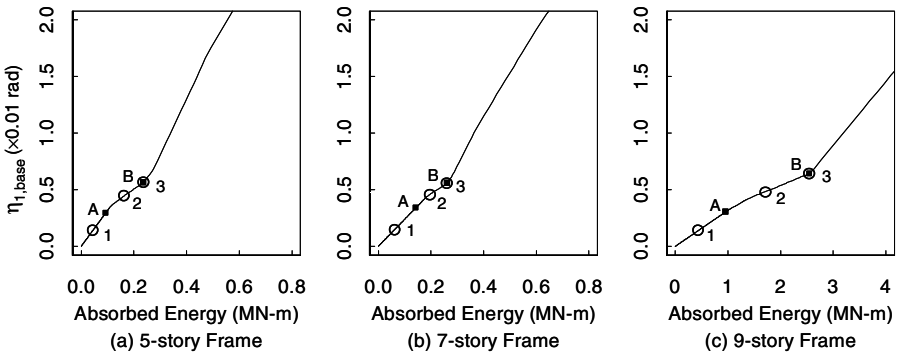

Figure 6 $\eta_{1,base}$ and Absorbed Energy Relationships

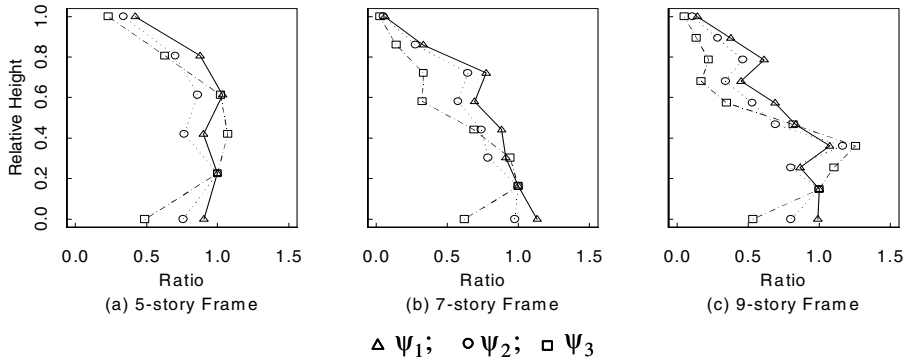

Figure 7 Energy Shape for first-mode Response

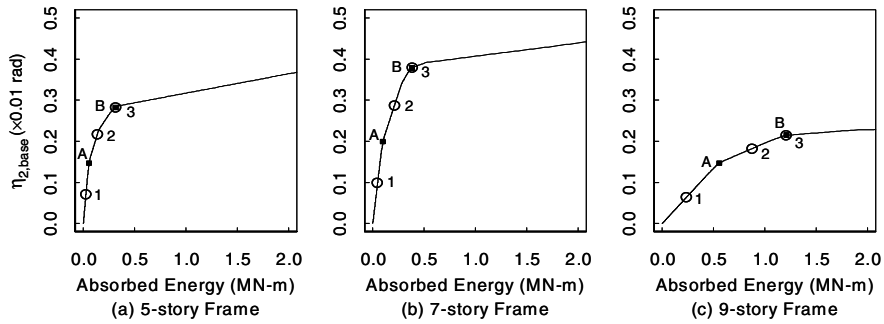

Figure 8 $\eta_{2,base}$ and Absorbed Energy Relationships

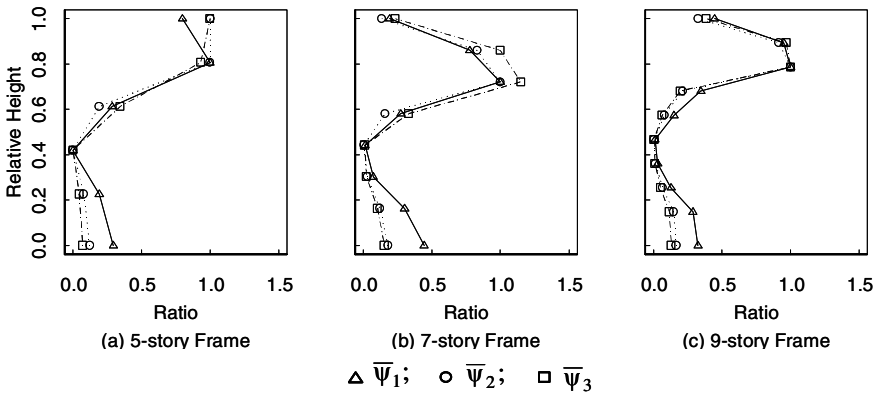

Figure 9 Energy Shape for second-mode Response

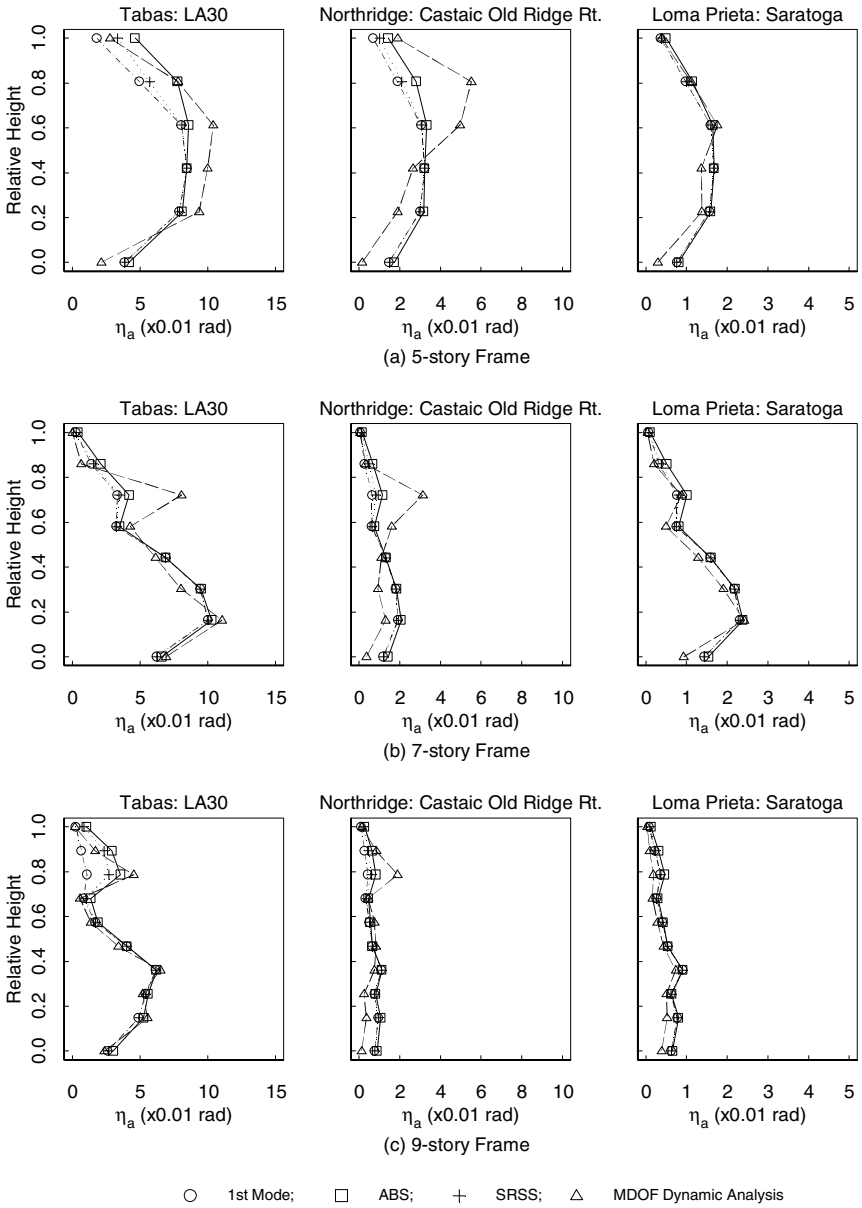

Figure 10 Comparison of η_a Distributions

CONCLUSIONS

A procedure, similar to the response spectrum method for elastic dynamic analysis, to compute the total energy demand from inelastic energy spectra and to distribute it along the height of a multistory frame is presented. The energy demand can be estimated without performing an inelastic time-history analysis. The procedure, which takes into account the higher mode effect for energy distribution in a low- to medium-rise frame, is summarized below.

(1) The MDOF frame is first converted into an equivalent SDOF system for each of the first two modes by elastic mode shapes.
(2) For each equivalent SDOF system, the generalized modal yield force is determined from a static pushover analysis with a lateral load (Eq. 8). Based on the modal yield strength coefficient and period, the modal ductility factor can be determined from the constant-ductility yield strength response spectrum [Figure 1(a)]. Based on the modal ductility factor, participation factor, and natural period, the absorbed energy of each mode is evaluated from the constant-ductility energy spectra [Figure 1(b)].
(3) Combination of the energy quantities in the first two modes by the absolute sum (ABS) rule provides a better estimation of the total energy demand than the SRSS rule.
(4) The absorbed energy of each mode is distributed along the frame height based on the specific energy shape (Eqs. 16 and 17), which is established from a static pushover analysis. The resulting energy distribution, expressed in the form of cumulative rotation, is the summation of contribution from each mode (Eqs. 18 or 19).

This study shows that the proposed procedure can predict the damage distribution of low- to medium-rise frames when response of the first two modes are considered (Figure 10). Although the majority of energy is contributed by the first mode, for some frames and earthquake ground motions used in this study the effect of second mode needs to be included to predict the damage in the upper stories.

REFERENCES

1. Fajfar P. and Gašperšič P. "The N2 method for the seismic damage analysis of RC buildings." *J. Earthquake Eng. Struct. Dyn.* 1996, 25, 31-46.
2. Chopra A. K. and Goel R. K. "A modal pushover analysis procedure to estimate seismic demands for buildings: theory and preliminary evaluation." *Report No. 2001/03*, Pacific Earthquake Engineering Research Center, University of California, Berkeley, CA, 2001.
3. Chou C. C. and Uang, C. M. "A procedure for evaluating seismic energy demand of framed structures." *J. Earthquake Eng. Struct. Dyn.* 2003, 32, 229-244.
4. Uang C. M. and Bertero V. V. "Evaluation of seismic energy in structures." *J. Earthquake Eng. Struct. Dyn.* 1990, 19(1), 77-90.
5. FEMA. "Recommended provisions for the development of seismic regulations for new Buildings." *FEMA-222A*, National Earthquake Hazards Reduction Program, Washington, D. C., 1997.
6. Somerville P. "Development of ground motion time histories for phase 2 of the FEMA/SAC steel project." *Report No. SAC/BD-97/04*, SAC Joint Venture, Sacramento, CA, 1997.
7. Chopra A. K. *Dynamics of structures: theory and applications to earthquake engineering*. Prentice Hall, New Jersey, 1995.
8. Krawinkler H. and Gupta A. "Story drift demands for steel moment frame structures in different seismic regions." *Proc. 6th U. S. National Conference on Earthquake Engineering*, Oakland, CA., 1998.